

## Statistical Distributions of Poisson Voronoi Cells in Two and Three Dimensions

Masaharu TANEMURA

*The Institute of Statistical Mathematics, 4-6-7 Minami-Azabu, Minato-ku, Tokyo 106-8569, Japan  
E-mail address: tanemura@ism.ac.jp*

(Received December 2, 2002; Accepted November 29, 2003)

**Keywords:** Delaunay Triangles, Generalized Gamma Distribution, Kiang's Conjecture, Maximum Likelihood Estimates, Voronoi Tessellation

**Abstract.** Statistical distributions of geometrical characteristics concerning the Poisson Voronoi cells, namely, Voronoi cells for the homogeneous Poisson point processes, are numerically obtained in two- and three-dimensional spaces based on the computer experiments. In this paper, ten million and five million independent samples of Voronoi cells in two- and three-dimensional spaces, respectively, are generated. Geometrical characteristics such as the cell volume, cell surface area and so on, are fitted to the generalized gamma distribution. Then, maximum likelihood estimates of parameters of the generalized gamma distribution are given.

### 1. Introduction

Tessellations of space for a given set of points into non-overlapping cells play an important role in the fields of science on form and stochastic geometry.

Among many possibilities of tessellations, the Voronoi tessellation might be the most popular and the most useful (see Fig. 1). The shape of cells of Voronoi tessellations clearly reflects the manner of configuration of points. Namely, some of the statistical properties of spatial point patterns are reflected into the properties of geometrical structure of the corresponding Voronoi tessellation. Thus, the Voronoi tessellation is playing an important role in the science on form.

From a point of view of application, the Voronoi cells are very useful as a geometrical model of crystal grains, biological cells, and so on. Voronoi cells are also useful as a tool for numerical computations.

We define the Poisson Voronoi cells as the typical Voronoi cell based on the homogeneous Poisson point processes. Recall that the homogeneous Poisson point process plays a role as the standard model for point patterns. Namely, statistical properties of Poisson point process are often used as the null hypothesis against the corresponding properties of competitive point process models.

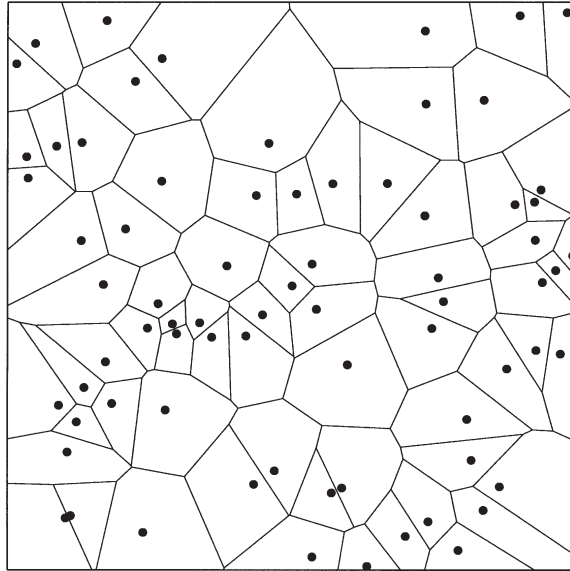


Fig. 1. A sample of Voronoi tessellation. Dotted points represent generating points. Polygon for each point is determined by the perpendicular bisectors between the point and its neighbouring points.

This situation is applicable to the Voronoi tessellation for the homogeneous Poisson point processes. Hence, it is important to know the statistical properties of Poisson Voronoi cells in order to compare the properties of Voronoi cells for other point patterns.

In spite of the above importance, the statistical properties of Poisson Voronoi cells are not much investigated, mainly because it is difficult to get them theoretically although some efforts to obtain expected values of certain kinds of properties have been done. Then, it needs an investigation with the aid of computer simulation.

In this paper, we present our results for the statistical distributions of Poisson Voronoi cells in two and three dimensional spaces. In the next section, previous efforts which had been made so far are briefly reviewed. In Section 3, we give the method which we applied in order to make independent samples of Poisson Voronoi cells. Section 4 shows the result of our computer simulations and the fitting several properties to the generalized gamma distribution. In the final section, we give some comments on our results together with previous results by other researchers.

## 2. Previous Works of Poisson Voronoi Cells

Much work has been done on this subject so far from theoretical point of view and from the simulation based aspect. Until now, theoretically known results about the properties of Poisson Voronoi cells are not enough from our stand point of getting their statistical distributions. For an example, let us consider the number of edges  $N$  of a Poisson Voronoi cell in the plane. It is known that  $E[N] = 6$  holds asymptotically (this is valid for a Voronoi

cell of any stochastic point processes). But the probability density which  $N$  for Poisson Voronoi cells should obey is not theoretically known yet. The situation is similar for other characteristic (let it be  $X$ ) of Poisson Voronoi cells and, in most cases, its statistical properties are partly known through the few lower moments such as  $E[X]$ ,  $E[X^2]$  and so on (see MØLLER (1994), for instance, as a review of mainly the theoretical aspect).

In order to investigate the spatial statistics of point patterns by using Voronoi cells, it is desirable to know all of the statistical properties of Poisson Voronoi cells as the standard. For that purpose, we inevitably take a computer simulation approach. There are many efforts in this direction, but we mention here only a few. HINDE and MILES (1980) have conducted a computer simulation of Poisson Voronoi cells in two dimensional space. The number of samples of their simulation was two million, which has been a record until now. As the characteristics of Poisson Voronoi polygons, HINDE and MILES (1980) reported the number of edges  $N$ , the area  $A$ , the perimeter  $S$  and the internal angle  $\theta$  of a typical cell. They obtained the first four moments of  $N$ ,  $A$ ,  $S$  and  $\theta$ , and then fitted their histograms to the three-parameter generalized gamma density.

In case of three-dimensional Poisson Voronoi cells, TANEMURA (1988) reported the statistical properties such as the distribution of the volume  $V$  and the number of faces  $F$  based on a hundred thousand sample of Voronoi polyhedra. More recently, KUMAR *et al.* (1992) presented the results of properties of three-dimensional Poisson Voronoi tessellation based on 358,000 simulated cells. They reported on the statistical properties of  $F$ ,  $V$ ,  $S$  (surface area),  $B$  (total edge length) of a Poisson Voronoi polyhedron and fitted their histograms to the two-parameter generalized gamma density. Note the term “density” used here is meant by the “probability density function”. We often use this notation throughout this paper.

### 3. Methods

In order to make independent samples of Voronoi cells for homogeneous Poisson processes, we use the following method. Although the two-dimensional terminology is used, the extension to other dimensions will be easy.

First, let  $R$  be the region where the generating points are distributed,  $|R|$  be the area of the region. Let  $\rho$  be the intensity of the Poisson point process. We generate a homogeneous Poisson point pattern inside  $R$  with intensity  $\rho$ . Then, the number of points inside  $R$  will obey the Poisson distribution with mean  $\rho|R|$ . Next, we select a point at random among the distributed points and construct a Voronoi cell of the selected point. Details of the procedure are the following:

(1) Letting  $n$  be the total number of independent samples, we set the number of points,  $m$ , inside  $R$  according to the Poisson distribution with mean  $\rho|R|$  theoretically for each sampling. Then, we generate  $m$  points inside  $R$  uniformly at random.

(2) Select a point at random among  $m$  points. Move the selected point to the center of the region  $R$  by keeping relative positions to other points by translations and by applying periodic boundary conditions. Then, construct the Voronoi polygon of the central point (see Fig. 2). If the union of circumcircles of Delaunay triangles which include the central point as one of vertices is included in  $R$  (see Fig. 3), the process for this sampling ends, otherwise we extend the region  $R$  (let the extended region be  $R'$ ) and generate a new set of

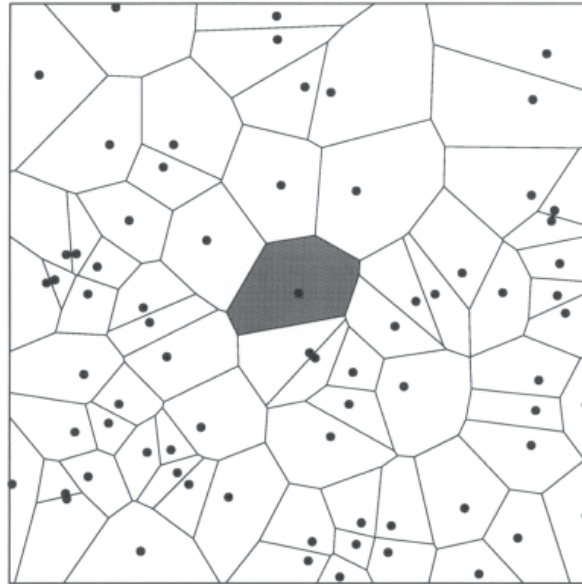


Fig. 2. A sample of Poisson Voronoi cell. Shaded polygon is the Voronoi polygon which is successfully made.

points with the same intensity  $\rho$ , select a central point, move other points such that the selected point is at the center of  $R'$  by applying the same procedure as above, and then construct the Voronoi polygon of central point. Repeat the process until the union of circumcircles of Delaunay triangles satisfy the above condition.

This procedure is basically due to HINDE and MILES (1980). In the paper of HINDE and MILES (1980), they have set  $\rho = 100$  in two-dimensional case. In the present simulations, we set  $\rho = 200$  for two-dimensional space, and  $\rho = 500$  for three-dimensional space. By these settings, the process of extension of the region  $R$  in the second step of the above procedure did not actually happen.

#### Algorithm for constructing Voronoi cell of the central point

Let us mention about the details of the algorithm for constructing the central Voronoi cell by using the example of two-dimensional space. Let us remind, for each realization of homogeneous Poisson point patterns, we are interested to construct a Voronoi polygon for a single central point as indicated by the shaded area in Fig. 2.

For that purpose, the algorithm devised by TANEMURA *et al.* (1983) is the most suitable. In their algorithm, all of the Delaunay triangles which include the central point as a vertex are efficiently constructed (see Fig. 3, for example). The computational complexity of this algorithm for constructing a single Voronoi polygon is  $O(m)$ , where  $m$  is the existing number of points in the current point pattern.

Here, we recall a set of efficient algorithms which are based on the results of the field of 'computational geometry' (see, for the existing algorithms OKABE *et al.* (2000), for

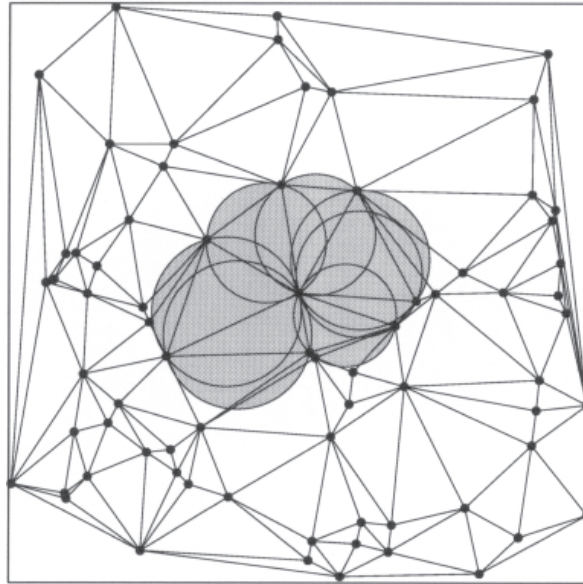


Fig. 3. A sample of Delaunay triangles corresponding to the Poisson Voronoi cell in Fig. 2. Lightly shaded circles represent the union of circumscribing circles of Delaunay triangles which construct the central Voronoi cell.

instance). The computational complexity of most of them is known as  $O(m \log m)$  for constructing all of the Voronoi polygons for a given point pattern. They are surely efficient for the tessellation by Voronoi polygons. However, most of the algorithms based on the computational geometry construct Voronoi cells of respective points by the incremental method or by the divide-and-conquer method. This means that, according to them, the proper Voronoi cell of a specified point is obtained only in the final step after  $O(m \log m)$  operations have been done.

Thus, the algorithm by TANEMURA *et al.* (1983) is suitable and sufficiently effective for our purpose.

#### 4. Results

##### 4.1. Poisson Voronoi cells in two dimensions

As was indicated, we have done a simulation of two-dimensional Poisson Voronoi cells with ten million independent samples, namely,  $n = 10,000,000$ . This value of  $n$  was selected in order to get more information about the statistical properties of Poisson Voronoi cells than the results of HINDE and MILES (1980) where  $n = 2,000,000$  was used.

Our results are classified into three categories:

1. Histograms of the reduced area  $a$ , the reduced perimeter  $s$ , the number of edges  $N$  of Poisson Voronoi cells. Here, the reduced area  $a$  is defined by  $a = \rho A$ ,  $A$  being the area of a Voronoi cell. Then, we can expect  $E[a] = 1$ . The reduced perimeter  $s$  is determined by

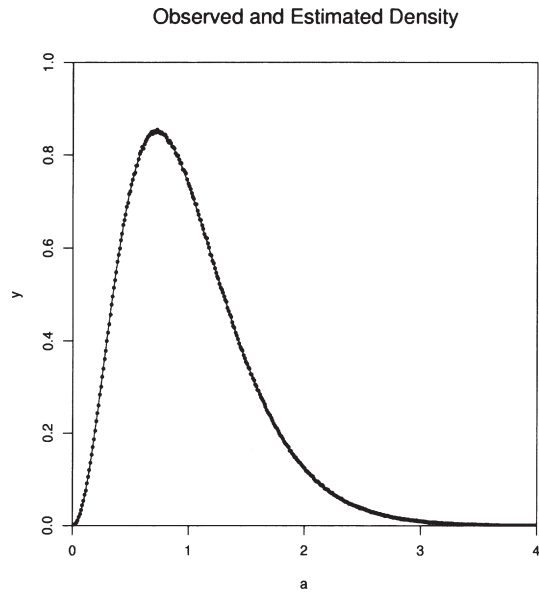


Fig. 4. Observed histogram of the reduced area of 2D Poisson Voronoi cells for ten million samples (dots) and its estimated probability density (line).

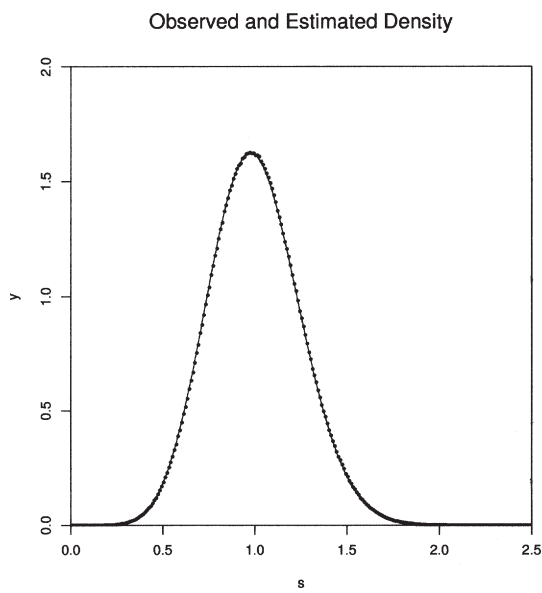


Fig. 5. Observed histogram of the reduced perimeter of 2D Poisson Voronoi cells for ten million samples (dots) and its estimated probability density (line).

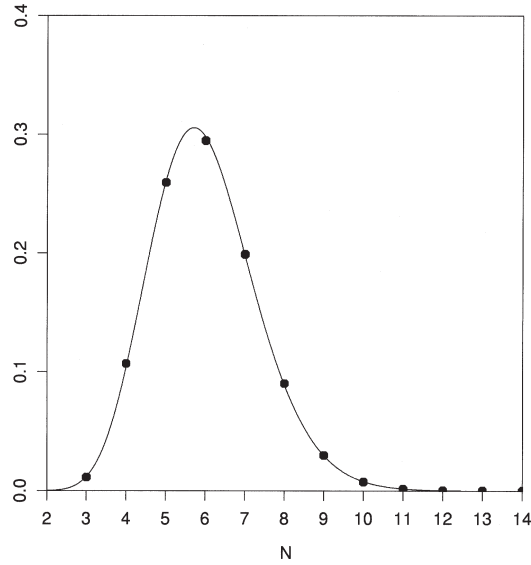


Fig. 6. Observed and estimated histogram of the number of edges of 2D Poisson Voronoi cells .

the relation  $s = \sqrt{\rho} S/4$ , where  $S$  is the perimeter of a Voronoi cell. In this case, we can expect also  $E[s] = 1$ , since it is known that, for a homogeneous Poisson point process,  $E[S] = 4/\sqrt{\rho}$  holds (MILES, 1970).

Also histograms of the area  $a_N$  and the perimeter  $s_N$  of Poisson Voronoi cells for a given number of edges are given.

2. Moments of  $a, s, N$ , and  $a_N$ .
3. Parameters  $a, b, c$  of generalized Gamma distribution

$$f(x|a, b, c) = \frac{ab^{c/a}}{\Gamma(c/a)} x^{c-1} \exp(-bx^a) \quad (a, b, c > 0) \tag{1}$$

fitted to the histograms of  $a, s, N, a_N$  and  $s_N$ .

**Histograms**

Dotted points in Figs. 4 and 5 represent the observed histograms of, respectively, the area  $a$  and the perimeter  $s$  of two-dimensional Poisson Voronoi cells. The class intervals for  $a$  and  $s$  were chosen as 0.01 which gave 700 classes for  $a$  and 300 classes for  $s$ . It is because the observed minimum and the maximum values of  $a$  and  $s$  were, respectively,  $a_{\min} = 0.002059$  and  $a_{\max} = 6.265011$  and  $s_{\min} = 0.059381$  and  $s_{\max} = 2.439198$ .

Moreover, dotted points in Fig. 6 indicate the histogram of observed number of edges  $N$  of Poisson Voronoi cells. In Table 1, the histograms of  $N$  for the present result together with the result of HINDE and MILES (1980) are given.

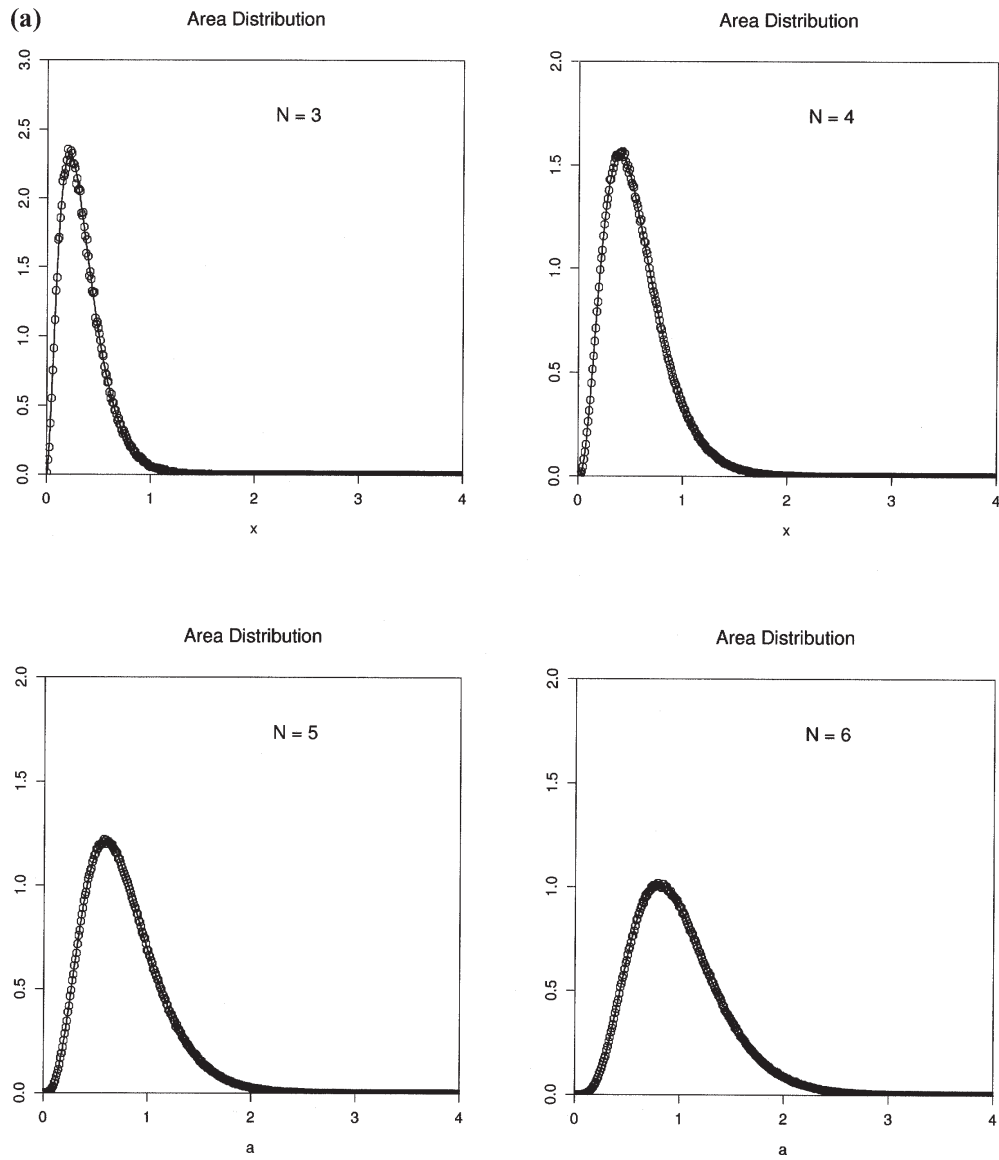


Fig. 7. (a) Observed histogram (open circle) and estimated density (line) of the area of 2D Poisson Voronoi cells for the number of edges 3, 4, 5, and 6. (b) Observed histogram (open circle) and estimated density (line) of the area of 2D Poisson Voronoi cells for the number of edges 7, 8, 9, and 10.



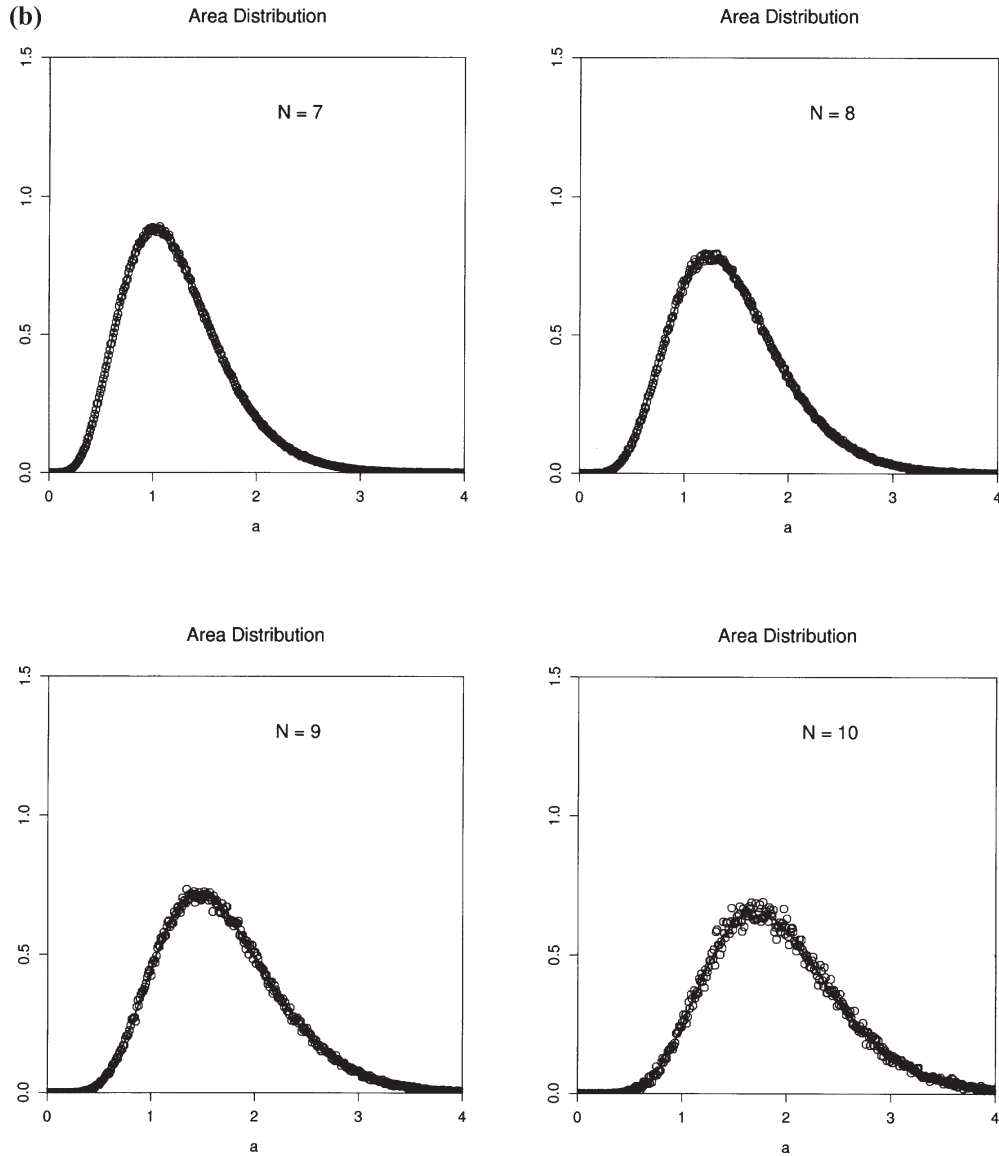


Fig. 7. (continued).

Open circles in Figs. 7a and 7b show the observed histograms of the area of 2-D Poisson Voronoi cells for respective number of edges  $N$ .

**Comparison of  $p_N$  for  $N = 3$  between the observation and theoretical computation**

We observed, as can be seen in Table 1, that the relative frequency  $p_N$  for  $N = 3$  is about

Table 1. Number of edges of 2-D Poisson Voronoi cell.

$N$	$n_N$	$\hat{p}_N$	$\hat{p}_N$ (HINDE and MILES, 1980)
3	112459	0.01125	0.01131
4	1068516	0.10685	0.1071
5	2594112	0.25941	0.2591
6	2947884	0.29479	0.2944
7	1988422	0.19884	0.1991
8	900262	0.09003	0.0902
9	296342	0.02963	0.0295
10	74261	0.00743	0.00743
11	14925	0.00149	0.00149
12	2462	0.00025	0.00025
13	312	0.00003	0.00003
14	39	0.00000	0.00000
15	4	0.00000	0.00000
16	0	0.00000	0.00000

$p_3 \sim 0.01125$  by our simulation result. Recently, HAYEN and QUINE (2000a, b) presented an integral formula for  $p_3$ , namely, the proportion of triangles in a Poisson Voronoi tessellation.

By numerical integration of the formula, they first obtained a value  $p_3 \sim 0.0112354$  to 7 decimal places (HAYEN and QUINE, 2000a) by performing five-fold integrations. In their subsequent paper (HAYEN and QUINE, 2000b), a revised value of

$$p_3 \sim 0.0112400129$$

to 10 decimal places was obtained by reducing the number of variables.

It is interesting that the above value of  $p_3$  is quite coincident with our corresponding value in Table 1. This result suggests the validity of our simulation of 2-D Poisson Voronoi cells.

### Estimated moments

The first four moments of variables  $N$ ,  $a$  and  $s$  are obtained as given in Tables 2a–c. In Tables 2a–c,  $\mu_k'$  of a random variable  $X$  are defined by  $\mu_k' \equiv E[X^k]$  ( $k = 1, 2, \dots$ ) and  $\mu_k$  are defined by  $\mu_k \equiv E[(X - \mu)^k]$  for  $k = 2, 3, \dots$ , where  $\mu = E[X]$ . Also the skewness  $\beta_1$  and the kurtosis  $\beta_2$  are defined, respectively, by  $\beta_1 = \mu_3/\sigma^3$  and  $\beta_2 = \mu_4/\sigma^4 - 3$ , where  $\sigma^2 = \mu_2$  is the variance.

Let us note that for the number of edges, we can expect  $E[N] = 6$  asymptotically (see for example, MILES (1970)). As regards the second moment  $\mu_2'$  of reduced area  $a$ , GILBERT (1962) has presented a formula which includes a double integral and has given the value  $\mu_2' = 1.280$  by numerical integration. We notice its agreement with our value  $\mu_2' = 1.28031$  in Table 2b.

Tables 3a and 3b show the moments of the area of 2-D Poisson Voronoi cells conditioned on the number of edges  $N$  (see Figs. 7a and 7b for their histograms). Table 3a

Table 2(a). Estimated moments of the number of edges  $N$  of 2-D Poisson Voronoi cells in comparison with the result of HINDE and MILES (1980).

	Present	HINDE and MILES (1980)
$\mu_1'$	5.99984	5.9997
$\mu_2'$	37.77860	37.778
$\mu_3'$	249.06111	249.07
$\mu_4'$	1715.31919	1715.4
$\sigma$	1.334350	1.335
$n^{-1.2}\sigma$	0.000422	0.00094
$\beta_1$	0.43360	0.432
$\beta_2$	0.20702	0.206

Table 2(b). Estimated moments of the reduced area  $a$  of 2-D Poisson Voronoi cells in comparison with the result of HINDE and MILES (1980).

	Present	HINDE and MILES (1980)
$\mu_1'$	1.00006	1.000217
$\mu_2'$	1.28031	1.2812
$\mu_3'$	1.99303	1.9969
$\mu_4'$	3.64852	3.6638
$\sigma$	0.52933	0.5299
$n^{-1.2}\sigma$	0.000167	0.00037
$\beta_1$	1.02640	1.033
$\beta_2$	1.55980	1.599

Table 2(c). Estimated moments of the reduced perimeter  $s$  of 2-D Poisson Voronoi cells in comparison with the result of HINDE and MILES (1980).

	Present	HINDE and MILES (1980)
$\mu_1'$	1.000052	1.000092
$\mu_2'$	1.05922	1.0594
$\mu_3'$	1.18023	1.1807
$\mu_4'$	1.37622	1.3772
$\sigma$	0.24313	0.2433
$n^{-1.2}\sigma$	0.000077	0.00017
$\beta_1$	0.18959	0.193
$\beta_2$	-0.02234	-0.017

Table 3(a). Estimated moments of the area  $a_N$  of 2-D Poisson Voronoi cells for given number of edges  $N$ .

$N$	3	4	5	6
$n_N$	112459	1068516	2594112	2947884
$\mu_1'$	0.34479	0.55810	0.77420	0.99621
$\mu_2'$	0.16325	0.40137	0.73723	1.18061
$\mu_3'$	0.09883	0.35501	0.83592	1.62589
$\mu_4'$	0.07324	0.37380	1.10209	2.55601
$\sigma$	0.21063	0.29982	0.37128	0.43379
$n^{-1.2}\sigma$	0.00063	0.00029	0.00023	0.00025
$\beta_1$	1.27827	1.13780	1.01056	0.91678
$\beta_2$	2.58398	1.99061	1.57440	1.30334

Table 3(b). Estimated moments of the area  $a_N$  of 2-D Poisson Voronoi cells for given number of edges  $N$ .

$N$	7	8	9	10
$n_N$	1988422	900262	296342	74261
$\mu_1'$	1.22181	1.45418	1.68690	1.92214
$\mu_2'$	1.73336	2.40957	3.19728	4.10391
$\mu_3'$	2.80500	4.48590	6.73178	9.64369
$\mu_4'$	5.10613	9.27567	15.59465	24.74464
$\sigma$	0.49043	0.54307	0.59301	0.63977
$n^{-1.2}\sigma$	0.00035	0.00057	0.00109	0.00235
$\beta_1$	0.84271	0.77537	0.72819	0.69470
$\beta_2$	1.10344	0.90388	0.78615	0.71529

is for  $a_N$  where  $N = 3, 4, 5$  and  $6$ , while Table 3b is the moments of  $a_N$  for  $N = 7, 8, 9$  and  $10$ .

### Fitting the generalized gamma distribution to the histograms

We tried to fit the observed histograms of various geometrical quantities of 2-D Poisson Voronoi cells to a certain flexible density function with a few parameters. Among a vast possibilities, we have selected the three-parameter generalized gamma distribution (1) since it will represent a wide range of distribution with a single mode and with an exponential decay for a large value. Moreover, that the range of its variable is limited to  $(0, \infty)$  is suitable for our purpose, since we are concerned with variables which take only positive values.

In order to estimate the parameters of the three-parameter generalized gamma distribution, we adapted the maximum likelihood estimation. Let  $L(a, b, c | \{X\})$  be the log-likelihood of parameters  $a, b$  and  $c$  for the observed data  $\{X\}$ . Then, we get for the generalized gamma distribution,

$$\begin{aligned}
 L(a, b, c|\{X\}) &= \log \prod_{i=1}^n f(x_i|a, b, c) \\
 &= \sum_{i=1}^n \log f(x_i|a, b, c) \\
 &= \sum_{i=1}^n \left\{ \log \frac{ab^{c/a}}{\Gamma(c/a)} + (c-1) \log x_i - bx_i^a \right\} \\
 &= n \log \frac{ab^{c/a}}{\Gamma(c/a)} + (c-1) \sum_{i=1}^n \log x_i - b \sum_{i=1}^n \log x_i^a.
 \end{aligned}$$

Let us define a new log-likelihood  $l$  divided by the number of samples  $n$ , by  $l = L/n$ , namely

$$\begin{aligned}
 l(a, b, c|\{X\}) &= \frac{1}{n} L(a, b, c|\{X\}) \\
 &= \log \frac{ab^{c/a}}{\Gamma(c/a)} + (c-1) \frac{1}{n} \sum_{i=1}^n \log x_i - b \frac{1}{n} \sum_{i=1}^n \log x_i^a.
 \end{aligned}$$

For the grouped data, the original data  $\{X\} = \{x_i\}$  ( $i = 1, 2, \dots, n$ ) is replaced by  $\{x_k, f_k\}$  ( $k = 1, 2, \dots, h$ ), where  $x_k$  is the representative values of the class  $k$ ,  $f_k$  the observed frequency in that class, and  $h$  is the number of classes. Then, our log-likelihood function of the grouped data for the generalized gamma distribution (1) tends to

$$l(a, b, c|\{x_k, f_k\}) = \log \frac{ab^{c/a}}{\Gamma(c/a)} + (c-1) \sum_{k=1}^h \frac{f_k}{n} \log x_k - b \sum_{k=1}^h \frac{f_k}{n} \log x_k^a.$$

We have estimated parameters  $(a, b, c)$  by numerically maximizing the above log-likelihood function for the grouped data. For the optimization, the quasi-Newton method was used.

Although the generalized gamma distribution is suitable for the random variables taking continuous positive values, we also applied it to the random variable which takes discrete positive values. Thus, we have done the above estimation procedure for the distributions of variables  $a, s, N, a_N$ , and  $s_N$ .

Tables 4a–c show the estimated parameters fitted to the area  $a$ , the perimeter  $s$  and the number of edges  $N$ , respectively, of 2-D Poisson Voronoi cells. In each table, the estimates by HINDE and MILES (1980) are also included for the comparison.

The line curves in Figs. 4 and 5 respectively are the estimated density for  $a$  and  $s$ . The line curve in Fig. 6 is the estimated relative frequency of  $N$ .

Tables 5a and 5b show the estimates of parameter values, respectively, of the area  $a_N$  and of the perimeter  $s_N$  of two-dimensional Poisson Voronoi cells conditioned on the

Table 4(a). Estimated parameters of the three-parameter generalized gamma distribution fitted to the area  $a$  of 2-D Poisson Voronoi cells. The values in the last row are the result by HINDE and MILES (1980) who fitted the same distribution. The last column ' $\chi^2$ (d.f.)' indicates the  $\chi^2$  values between the observed frequencies of our computer simulation and the expected frequencies derived from the estimated parameter values of generalized gamma distribution. 'd.f.' is the degree of freedom of  $\chi^2$  distribution.

	$\hat{a}$	$\hat{b}$	$\hat{c}$	$\chi^2$ (378)
Present	1.07950	3.03226	3.31122	638.6
HINDE and MILES (1980)	1.0787	3.0328	3.3095	646.5

Table 4(b). Estimated parameters of the three-parameter generalized gamma distribution fitted to the perimeter  $s$  of 2-D Poisson Voronoi cells. The values in the last row are the result by HINDE and MILES (1980) who fitted the same distribution. For the meaning of the last column ' $\chi^2$ (d.f.)', see the legend in Table 4a.

	$\hat{a}$	$\hat{b}$	$\hat{c}$	$\chi^2$ (181)
Present	2.33609	2.97006	7.58060	917.9
HINDE and MILES (1980)	2.3389	2.9563	7.5579	937.3

Table 4(c). Estimated parameters of the three-parameter generalized gamma distribution fitted to the number of edges  $N$  of 2-D Poisson Voronoi cells. The values in the last row are the result by HINDE and MILES (1980) who fitted the same distribution.

	$\hat{a}$	$\hat{b}$	$\hat{c}$
Present	0.96853	3.80078	20.86016
HINDE and MILES (1980)	1.0186	3.130	19.784

number of edges  $N$ . The line curves in Figs. 7a and 7b indicate the estimated density of  $a_N$  for respective values of  $N = 3, \dots, 10$ . These results, together with those for  $a$ ,  $s$  and  $N$ , suggest that the three-parameter generalized gamma distribution (1) is capable to fit a wide range of propability density of geometrical quantities as presented here.

#### 4.2. Poisson Voronoi cells in three dimensions

In three dimensions, we have set  $\rho = 500$  as was indicated and have done a simulation of three-dimensional Poisson Voronoi cells with five million independent samples, namely,  $n = 5,000,000$ . This value of  $n$  was selected in order to get more information about the statistical properties of Poisson Voronoi cells than the results of KUMAR *et al.* (1992) where  $n = 358,000$  was used.

Our results are classified into three categories as in the 2-D case:

1. Histograms of the reduced volume  $v$ , the reduced surface area  $s$ , the number of faces  $F$  of Poisson Voronoi cells. Here, the reduced volume  $v$  is defined by  $v = \rho V$ ,  $V$  being the volume of a Voronoi cell computed for the Poisson point process with intensity  $\rho$ . Then, we can expect  $E[v] = 1$ . The reduced surface area  $s$  is defined by the relation  $s = \rho^{2/3} S$ , where

Table 5(a). Estimated parameters of the area  $a_N$  of  $N$ -sided 2-D Poisson Voronoi cell.  $\hat{a}$ ,  $\hat{b}$ ,  $\hat{c}$  are the estimates of parameters in the generalized gamma distribution (1).

$N$	$n_N$	$\hat{a}$	$\hat{b}$	$\hat{c}$
3	112459	0.91104	8.64192	2.94215
4	1068516	0.88311	7.55504	3.93014
5	2594112	0.88753	7.01095	4.90362
6	2947884	0.89449	6.67685	5.90079
7	1988422	0.90242	6.40916	6.88220
8	900262	0.91634	6.09238	7.82694
9	296342	0.90563	6.17656	8.93527
10	74261	0.90592	6.11545	9.96771
11	14925	0.99382	4.76883	10.20898

Table 5(b). Estimated parameters of the perimeter  $s_N$  of  $N$ -sided 2-D Poisson Voronoi cell to the three-parameter generalized gamma density (1).

$N$	$n_N$	$\hat{a}$	$\hat{b}$	$\hat{c}$
3	112459	1.96044	5.90003	5.99042
4	1068516	1.93086	5.98970	8.05632
5	2594112	1.92828	5.96544	10.05676
6	2947884	1.92219	5.98215	12.10193
7	1988422	1.92241	5.97101	14.11393
8	900262	1.93152	5.89743	16.08546
9	296342	1.91499	5.99192	18.18228
10	74261	1.89139	6.18189	20.43442
11	14925	2.13233	4.51298	20.28079

$S$  is the surface area of a Voronoi cell for the Poisson point process with intensity  $\rho$ . In this case, we can expect also  $E[s] \sim 5.821$ , since it is known that, for a homogeneous Poisson point process,  $E[S] = (256\pi/3)^{1/3}\Gamma(5/3)\rho^{-2/3}$  holds (MEIJERING, 1953).

Also histograms of the volume  $v_F$  and the surface area  $s_F$  of Poisson Voronoi cells for a given number of faces are given.

2. Moments of  $v$ ,  $s$ ,  $F$ , and  $v_F$ .
3. Parameters  $a$ ,  $b$ ,  $c$  of generalized Gamma distribution

$$f(x|a, b, c) = \frac{ab^{c/a}}{\Gamma(c/a)} x^{c-1} \exp(-bx^a) \quad (a, b, c > 0)$$

fitted to the histograms of  $v$ ,  $s$ ,  $F$ ,  $v_F$  and  $s_F$ .

### Histograms

Dotted points in Figs. 8 and 9 show the observed histograms of, respectively, the volume  $v$  and the surface area  $s$  of three-dimensional Poisson Voronoi cells. The class

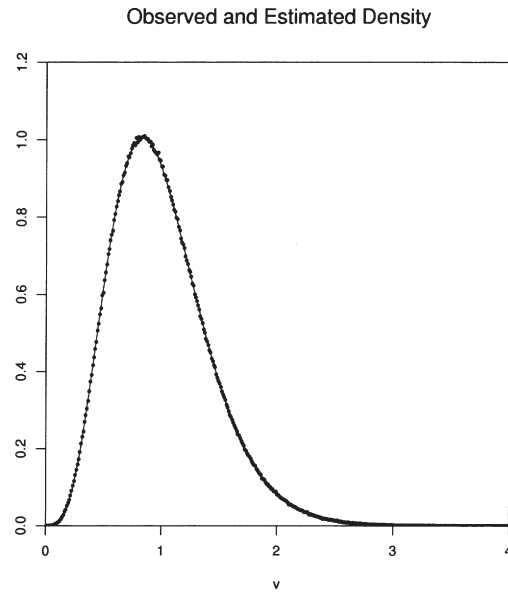


Fig. 8. Observed histogram (dots) of the volume of 3D Poisson Voronoi cells for five million samples and its estimated density (line).

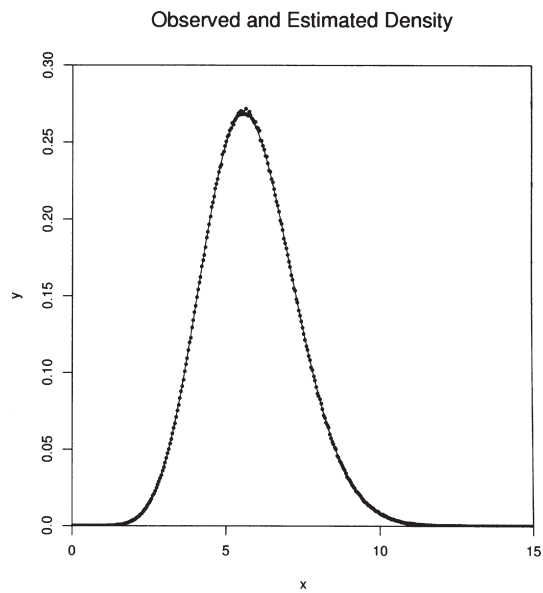


Fig. 9. Observed histogram (dots) of the surface area of 3-D Poisson Voronoi cells for five million samples and its estimated density (line).



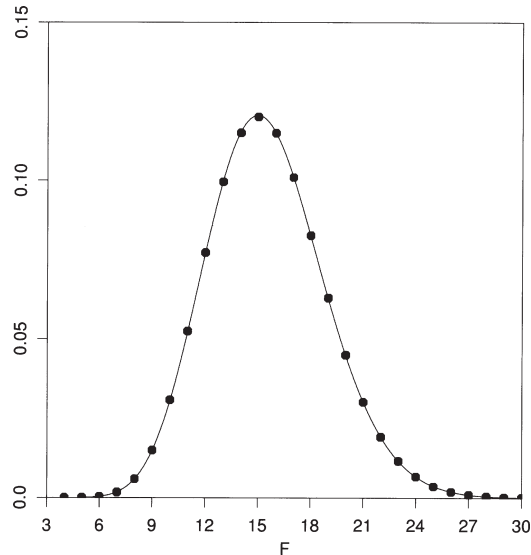


Fig. 10. Observed and estimated histogram of the number of faces of 3-D Poisson Voronoi cells.

intervals of  $v$  and  $s$  were respectively chosen to be 0.01 and 0.04, which gave 500 and 400 classes for  $v$  and  $s$ , respectively. It is because the observed minimum and maximum values of  $v$  and  $s$  were, respectively,  $v_{\min} = 0.015622$  and  $v_{\max} = 4.623616$ , and  $s_{\min} = 0.558396$  and  $s_{\max} = 14.812654$ .

Dotted points in Fig. 10 show the histogram of observed number of faces  $F$  of three-dimensional Poisson Voronoi cells. Table 6 gives the histogram of the number of faces  $F$  of 3-D Poisson Voronoi cells for our simulation of five million samples together with the relative frequencies  $\hat{p}_F$  obtained by KUMAR *et al.* (1992) which is based on 358,000 samples of 3-D Poisson Voronoi cells. In Table 6, the second column is  $n_F$ , the observed frequency, and the third column is the relative frequency  $\hat{p}_F$  for respective number of faces  $F$ . Let us remind that in the previous subsection, we have done a comparison between the observed relative frequency of  $p_N$  for  $N = 3$  and its theoretical estimate. In this three-dimensional case, however, the frequency for the possible minimum number of faces, namely,  $F = 4$ , is quite small. This point is a remarkable difference between two and three dimensional cases. Thus, it will be much more difficult to ascertain our result of computer simulation from the theoretical result of  $p_F$  for  $F = 4$ , even if  $p_F$  is obtained theoretically. In order to do the above comparison, more and more samples of 3-D Poisson Voronoi cells would be required.

Open circles in Figs. 11a, 11b and 11c show the observed histograms of the volume of 3-D Poisson Voronoi cells for respective number of faces  $F$ .

### Estimated moments

The first four moments of variables  $F$ ,  $v$  and  $s$  are respectively summarized in Tables

Table 6. Distribution of the number of faces  $F$  of 3-D Poisson Voronoi cell.

$F$	$n_F$	$\hat{p}_F$	$\hat{p}_F$ (KUMAR <i>et al.</i> , 1992)
4	5	0.000001	0.00001
5	201	0.000040	0.00003
6	1727	0.000345	0.00033
7	8630	0.001726	0.00159
8	29584	0.005917	0.00581
9	74893	0.014979	0.01494
10	154028	0.030806	0.03089
11	262323	0.052465	0.05212
12	386388	0.077278	0.07695
13	497897	0.099579	0.10041
14	575303	0.115061	0.11465
15	600757	0.120151	0.11927
16	574918	0.114984	0.11485
17	504944	0.100989	0.10144
18	413511	0.082702	0.08244
19	315057	0.063011	0.06325
20	225014	0.045003	0.04523
21	150740	0.030148	0.03062
22	95848	0.019170	0.01935
23	58143	0.011629	0.01164
24	33486	0.006697	0.00672
25	18079	0.003616	0.00382
26	9528	0.001906	0.00186
27	4789	0.000958	0.00975
28	2354	0.000471	0.00500
29	1031	0.000206	0.00198
30	460	0.000092	0.00061
31	228	0.000046	0.00039
32	82	0.000016	0.00014
33	29	0.000006	0.00003
34	15	0.000003	0.00006
35	3	0.000001	0.00000
36	3	0.000001	0.00000

7a–c. Similar notations of symbols for moments are used as in Tables 2a–c. As regards the mean value of  $F$ , it is known that

$$E[F] = \frac{48\pi^2}{35} + 2 = 15.535457\dots$$

by MEIJERING (1953). Concerning the second moment  $\mu_2'$  of reduced volume  $v$ , GILBERT (1962) has given the value  $\mu_2' = 1.180$  by numerical integration. We can observe its good agreement with our value  $\mu_2' = 1.17830$  in Table 7b.

Tables 8a–c are the estimated moment values of the volume  $v_F$  of three dimensional Poisson Voronoi cells conditioned on the number of faces  $F$ .

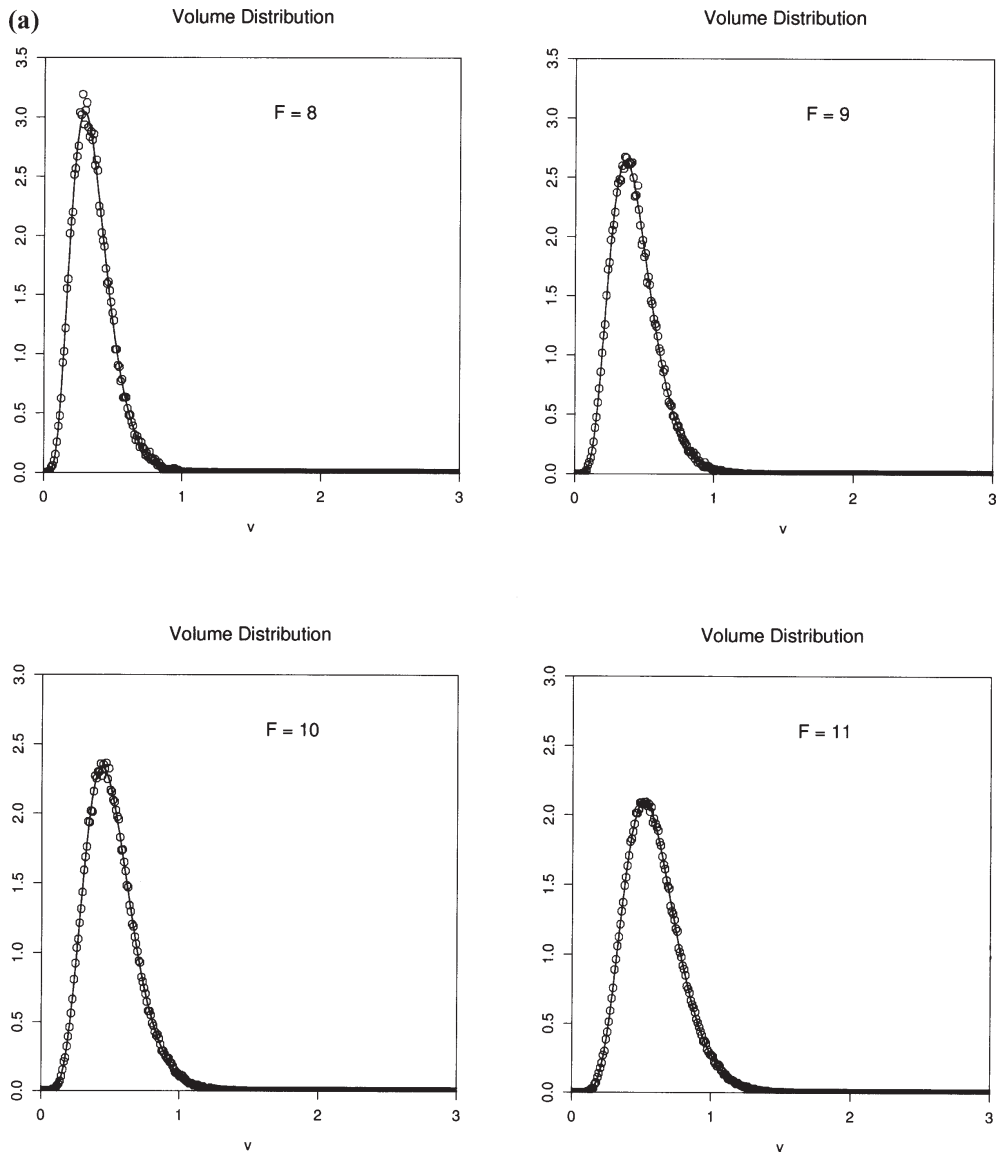


Fig. 11. (a) Observed histogram (open circle) and estimated density (line) of the volume of 3D Poisson Voronoi cells for the number of faces 8, 9, 10, and 11. (b) Observed histogram (open circle) and estimated density (line) of the volume of 3D Poisson Voronoi cells for the number of faces 12, 13, 14, and 15. (c) Observed histogram (open circle) and estimated density (line) of the volume of 3D Poisson Voronoi cells for the number of faces 16, 17, 18, and 19.

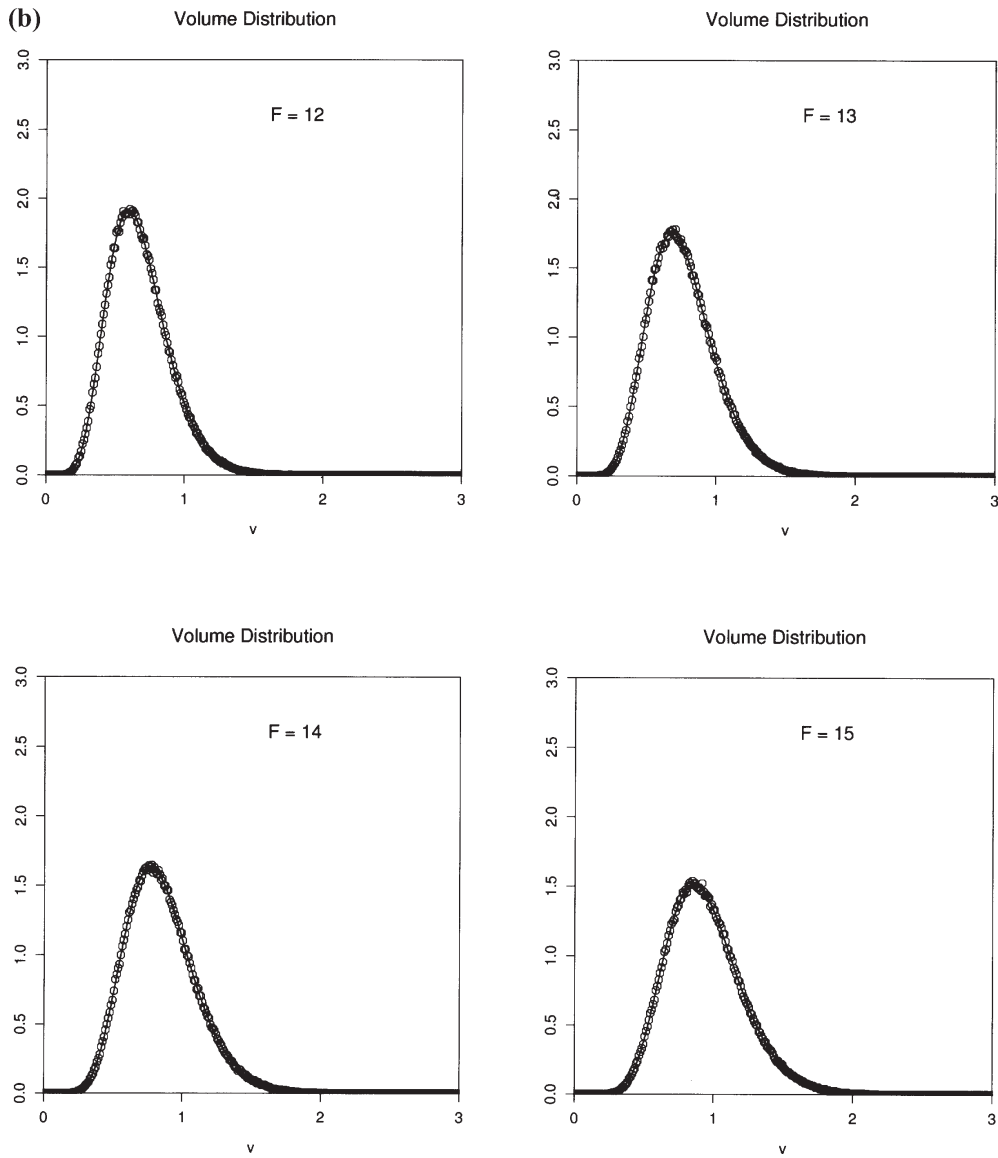


Fig. 11. (continued).

### Fitting the generalized gamma distribution to the histograms

We fitted the observed histograms of  $v$ ,  $s$ ,  $F$ ,  $v_F$  and  $s_F$  to the three-parameter gamma distribution of Eq. (1) as in the case of two-dimensions.

Tables 9a–c give the estimates of parameters of generalized gamma distribution fitted

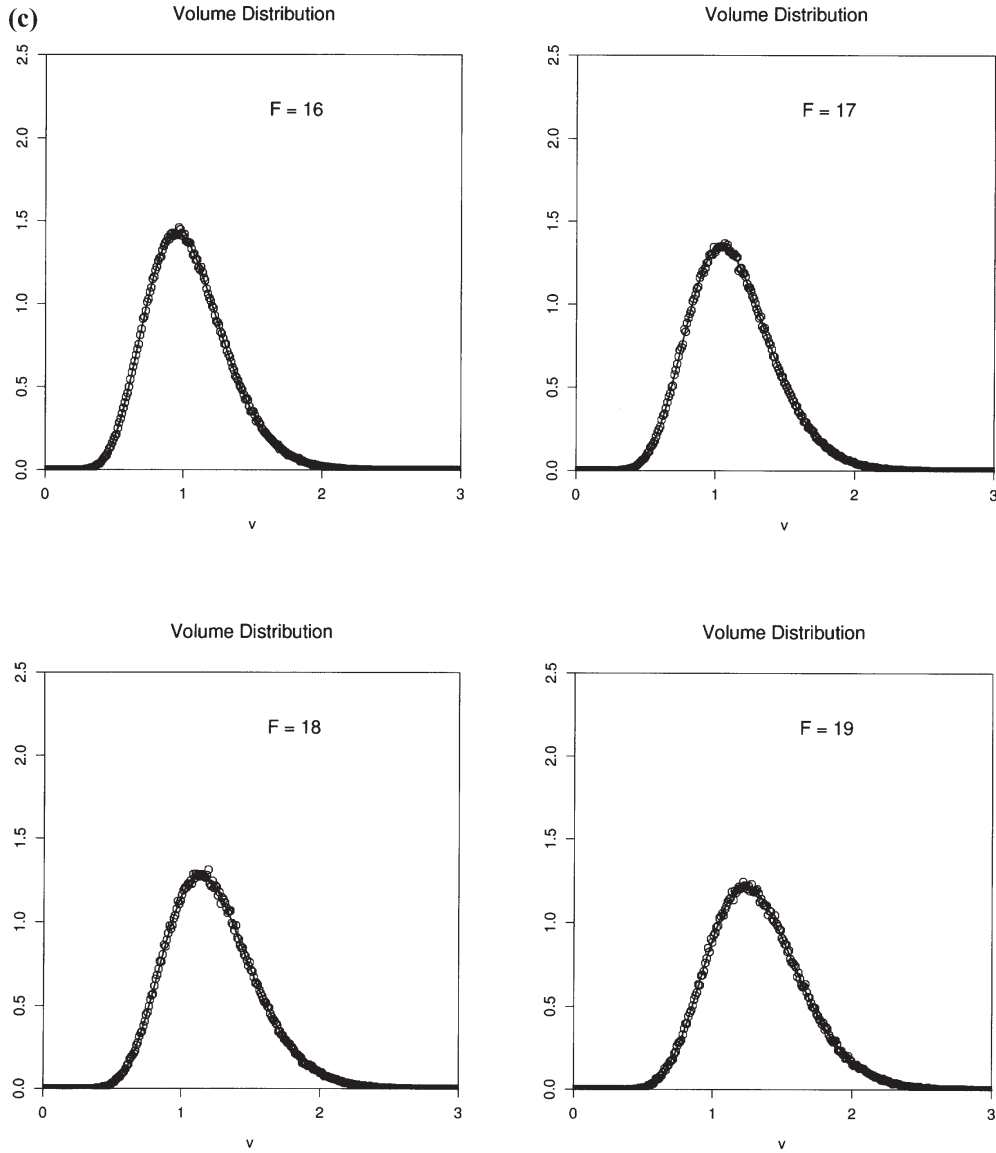


Fig. 11. (continued).

to the volume  $v$ , the surface area  $s$  and the number of faces  $F$ , respectively, of 3-D Poisson Voronoi cells. In each table, the estimates by KUMAR *et al.* (1992) are also included. Notice that KUMAR *et al.* (1992) have adopted the two-parameter generalized gamma fit (they used  $b$  and  $c$  as variable parameters by fixing  $a = 1$  in our Eq. (1)). Then, we independently fitted

Table 7(a). Estimated moments of the number of faces  $F$  of 3-D Poisson Voronoi cells in comparison with the result of KUMAR *et al.* (1992).

	Present	KUMAR <i>et al.</i> (1992)
$\mu_1'$	15.53215	15.5431
$\mu_2'$	252.35345	252.710
$\mu_3'$	4276.84510	—
$\mu_4'$	75421.60050	—
$\sigma$	3.33252	3.3350
$n^{-1/2}\sigma$	0.001490	0.00557
$\beta_1$	0.33133	0.3476
$\beta_2$	0.11292	0.0998

Table 7(b). Estimated moments of the reduced volume  $v$  of 3-D Poisson Voronoi cells in comparison with the result of KUMAR *et al.* (1992).

	Present	KUMAR <i>et al.</i> (1992)
$\mu_1'$	0.99974	1.0011
$\mu_2'$	1.17830	1.1784
$\mu_3'$	1.59478	—
$\mu_4'$	2.43247	—
$\sigma$	0.42286	0.4198
$n^{-1/2}\sigma$	0.000189	0.00070
$\beta_1$	0.78350	0.7874
$\beta_2$	0.88551	0.8108

Table 7(c). Estimated moments of the reduced surface area  $s$  of 3-D Poisson Voronoi cells in comparison with the result of KUMAR *et al.* (1992).

	Present	KUMAR <i>et al.</i> (1992)
$\mu_1'$	5.82003	5.8267
$\mu_2'$	36.06266	36.092
$\mu_3'$	236.36429	—
$\mu_4'$	1630.18262	—
$\sigma$	1.47985	1.4635
$n^{-1/2}\sigma$	0.000662	0.00245
$\beta_1$	0.30470	0.3098
$\beta_2$	0.07669	0.0464

Table 8(a). Estimated moments of the volume  $v_F$  of 3-D Poisson Voronoi cells for given number of faces  $F$ .

$F$	7	8	9	10	11	12
$n_F$	8630	29584	74893	154028	262323	386388
$\mu_1'$	0.27917	0.35291	0.42727	0.50640	0.58808	0.67239
$\mu_2'$	0.09291	0.14538	0.20951	0.29015	0.38692	0.50099
$\mu_3'$	0.03611	0.06872	0.11628	0.18594	0.28203	0.41033
$\mu_4'$	0.01612	0.03673	0.07224	0.13200	0.22586	0.36700
$\sigma$	0.12237	0.14435	0.16417	0.18360	0.20270	0.22109
$n^{-1/2}\sigma$	0.00132	0.00084	0.00060	0.00047	0.00040	0.00036
$\beta_1$	0.99040	0.89869	0.84351	0.78538	0.74020	0.71618
$\beta_2$	1.52407	1.21533	1.14520	0.97805	0.85368	0.84783

Table 8(b). Estimated moments of the volume  $v_F$  of 3-D Poisson Voronoi cells for given number of faces  $F$ .

$F$	13	14	15	16	17	18
$n_F$	497897	575303	600757	574918	504944	413511
$\mu_1'$	0.76015	0.84902	0.94099	1.03393	1.12915	1.22516
$\mu_2'$	0.63512	0.78642	0.96082	1.15347	1.36918	1.60528
$\mu_3'$	0.57913	0.78972	1.05890	1.38178	1.77543	2.24113
$\mu_4'$	0.57288	0.85501	1.25369	1.76977	2.45283	3.32298
$\sigma$	0.23935	0.25609	0.27453	0.29061	0.30693	0.32288
$n^{-1/2}\sigma$	0.00034	0.00034	0.00035	0.00038	0.00043	0.00050
$\beta_1$	0.67476	0.63464	0.62531	0.59171	0.57682	0.56319
$\beta_2$	0.73178	0.61467	0.61883	0.53219	0.52530	0.50585

Table 8(c). Estimated moments of the volume  $v_F$  of 3-D Poisson Voronoi cells for given number of faces  $F$ .

$F$	19	20	21	22	23	24
$n_F$	315057	225014	150740	95848	58143	33486
$\mu_1'$	1.32295	1.42171	1.52376	1.62332	1.72525	1.83095
$\mu_2'$	1.86479	2.14608	2.45844	2.78229	3.13440	3.52259
$\mu_3'$	2.79142	3.42914	4.18834	5.02134	5.98381	7.10588
$\mu_4'$	4.42431	5.78399	7.51614	9.51905	11.98045	15.00021
$\sigma$	0.33852	0.35331	0.36959	0.38357	0.39737	0.41256
$n^{-1/2}\sigma$	0.00060	0.00074	0.00095	0.00124	0.00165	0.00225
$\beta_1$	0.54612	0.52386	0.51472	0.48072	0.49959	0.46877
$\beta_2$	0.47523	0.41974	0.42210	0.35333	0.39527	0.35243

Table 9(a). Estimated parameters of the three-parameter generalized gamma distribution fitted to the volume  $v$  of 3-D Poisson Voronoi cells. Estimates of two-parameter generalized gamma fit ( $a = 1$ : fixed) by the present author and by KUMAR *et al.* (1992) are also given for the comparison.

	$\hat{a}$	$\hat{b}$	$\hat{c}$
Present	1.16788	4.04039	4.79803
2-param.	1.0 (fixed)	5.48854	5.48714
Kumar	1.0 (fixed)	5.6117	5.6333

Table 9(b). Estimated parameters of the three-parameter generalized gamma distribution fitted to the surface area  $s$  of 3-D Poisson Voronoi cells. Estimates of two-parameter generalized gamma fit ( $a = 1$ : fixed) by the present author and by KUMAR *et al.* (1992) are also given for the comparison.

	$\hat{a}$	$\hat{b}$	$\hat{c}$
Present	1.86256	0.16289	8.48552
2-param.	1.0 (fixed)	2.56162	14.90867
Kumar	1.0 (fixed)	2.6469	15.4847

Table 9(c). Estimated parameters of the three-parameter generalized gamma distribution fitted to the number of faces  $F$  of 3-D Poisson Voronoi cells. Estimates of two-parameter generalized gamma fit ( $a = 1$ : fixed) by the present author and by KUMAR *et al.* (1992) are also given for the comparison.

	$\hat{a}$	$\hat{b}$	$\hat{c}$
Present	1.44965	0.19187	15.05113
2-param.	1.0 (fixed)	1.37964	21.42884
Kumar	1.0 (fixed)	1.3891	21.6292

our simulation data to the two-parameter generalized gamma distribution in order to compare them with the results of KUMAR *et al.* (1992).

Estimated density of the volume  $v$  and of the surface area  $s$ , respectively, are indicated as line curves in Figs. 8 and 9. Estimated relative frequency of the number of faces  $F$  is shown in Fig. 10. These three curves are obtained from the three-parameter generalized gamma fit in Tables 9a–c. The results indicate each a nice fit to the observation. On the contrary, the two-parameter generalized gamma fits as given in Tables 9a–c, including the results of KUMAR *et al.* (1992), all showed a slight systematic deviation from our observed histograms.

Tables 10a and 10b show the estimates of three-parameter generalized gamma fit, respectively, of the volume  $v_F$  and of the surface area  $s_F$  of three-dimensional Poisson Voronoi cells conditioned on the number of faces  $F$ . The line curves in Figs. 11a, 11b and 11c indicate the estimated density of  $v_F$  for respective values of  $F = 8, \dots, 19$ . These results again suggest the capability of three-parameter generalized gamma fit to a wide range of probability density in our problem.



Table 10(a). Estimated parameters of the volume  $v_F$  of  $F$ -faced 3-D Poisson Voronoi cell to the three-parameter generalized gamma density (1).

$N$	$n_N$	$\hat{a}$	$\hat{b}$	$\hat{c}$
7	8630	0.82346	22.36141	6.35271
8	29584	0.80934	21.53615	7.40886
9	74893	0.80362	21.04668	8.44347
10	154028	0.85523	18.79045	8.90942
11	262323	0.85227	18.37213	9.88683
12	386388	0.85073	18.06106	10.88840
13	497897	0.87702	16.78236	11.51136
14	575303	0.89256	16.04023	12.31797
15	600757	0.86763	16.54518	13.55164
16	574918	0.89110	15.53634	14.20837
17	504944	0.88706	15.50650	15.26408
18	413511	0.87185	15.93744	16.52283
19	315057	0.87061	15.85851	17.55166
20	225014	0.88398	15.23324	18.32121
21	150740	0.88192	15.12351	19.27887
22	95848	0.96293	12.12578	18.59853
23	58143	0.83063	17.44704	22.71260

Table 10(b). Estimated parameters of the surface area  $s_F$  of  $F$ -faced 3-D Poisson Voronoi cell to the three-parameter generalized gamma density (1).

$N$	$n_N$	$\hat{a}$	$\hat{b}$	$\hat{c}$
7	8630	1.28948	2.08032	10.57979
8	29584	1.29581	1.99734	12.14340
9	74893	1.28241	2.05230	13.91442
10	154028	1.34905	1.67015	14.78239
11	262323	1.34420	1.67129	16.37906
12	386388	1.33630	1.69382	18.03030
13	497897	1.35515	1.57736	19.26449
14	575303	1.38620	1.42721	20.46514
15	600757	1.34297	1.60958	22.50512
16	574918	1.38092	1.42127	23.48764
17	504944	1.36730	1.47730	25.26716
18	413511	1.35422	1.53589	27.05244
19	315057	1.32554	1.68809	29.21512
20	225014	1.36272	1.48282	30.02826
21	150740	1.37970	1.38506	31.05803
22	95848	1.47641	0.98816	30.47677
23	58143	1.23021	2.38273	38.41532

## 5. Discussion

In the present paper, we have done computer simulations of Poisson Voronoi cells in two and three dimensional spaces. The numbers of independent samples generated were  $n = 10,000,000$  and  $n = 5,000,000$  for two-dimensions and for three-dimensions, respectively. These sample sizes are the biggest among the computer simulations so far reported.

Computer simulations of Poisson Voronoi cells of such a big size of random samples are now becoming possible to perform because of the recent increase of computer power. This circumstance is becoming obvious not only in the high-end computer environments, but also in the level of personal computers with lower cost.

One of the points which became clear from the results of the present computer simulation is the good coincidence between the observed relative frequency of triangles for the two-dimensional Poisson Voronoi cells and its theoretical estimate given by HAYEN and QUINE (2000a, b). This coincidence shows not only the validity of our simulation procedure, but also the necessity of large number of independent samples in the Monte Carlo simulation of Poisson Voronoi cells. Such a coincidence would not be obtained if the number of samples is less. This point shows, at the same time, the difficulty of performing theoretically the derivation of the distribution of the number of edges of Poisson Voronoi cells, even in two-dimensions.

Second point to be discussed is on our results of the estimated values of parameter of three-parameter generalized gamma fit to the area  $a$  in two-dimensions and to the volume  $v$  in three-dimensions. We refer their values here again together the corresponding values in one-dimension as follows:

Dimension	$\hat{a}$	$\hat{b}$	$\hat{c}$
1	1.0 (exact)	2.0 (exact)	2.0 (exact)
2	1.07950	3.03226	3.31122
3	1.16788	4.04039	4.79803

Here, the size (namely, the length)  $x$  of one-dimensional Poisson Voronoi cell is known to obey the following density:

$$f(x) = 4x \exp(-2x),$$

which indicates that the parameters of Eq. (1) give the values of  $a = 1$ ,  $b = 2$  and  $c = 2$  in this case.

From the above table, we immediately note that there might exist some relationship among parameters on the dimensionality of space. In relation to this point, we recall "Kiang's conjecture" (KIANG, 1966). He conjectured based on his Monte Carlo simulation of 2-D and 3-D random Voronoi tessellations, that the probability distribution of the volume  $x$  of the Voronoi cell is of the form:

$$f(x) = \frac{\alpha}{\Gamma(\alpha)} (\alpha x)^{\alpha-1} \exp(-\alpha x); \quad \alpha = 2d$$

where  $d$  is the dimension of space. Later, the Kiang's conjecture was denied by TANEMURA (1988) through his computer simulation of 3-D Poisson Voronoi tessellation. In TANEMURA (1988),  $n = 100,000$  Voronoi cells are randomly sampled from fifty independent realizations of 4000 point Poisson point processes. Then, the empirical distribution of the volume of Voronoi cells was fitted to the three-parameter generalized gamma distribution (1) using a non-linear least-squares method. The estimated values of parameters were  $\hat{a} = 1.409$ ,  $\hat{b} = 2.813$  and  $\hat{c} = 4.120$ , which showed a discrepancy from the Kiang's conjecture, namely,  $a = 1$ ,  $b = 4$  and  $c = 4$ . It will be clear that the above estimated values of present investigation again reject Kiang's conjecture. However, we note there might be a certain tendency between the parameter values and the dimension of space as was stated. Thus, it will be interesting to investigate the Poisson Voronoi cells in higher dimensions.

This research was partly supported by the Grant-in-Aid for Scientific Research (C) No. 10680326 and No. 13680379 from the Ministry of Education, Science, Sports and Culture of Japan. The author is also grateful to the referee whose comments were helpful to improve the manuscript.

#### REFERENCES

- GILBERT, E. N. (1962) Random subdivision of space into crystals, *Annals of Math. Statist.*, **33**, 958–972.
- HAYEN, A. and QUINE, M. (2000a) The proportion of triangles in a Poisson-Voronoi tessellation of the plane, *Advances in Appl. Prob. (SGSA)*, **32**, 67–74.
- HAYEN, A. and QUINE, M. (2000b) Calculating the proportion of triangles in a Poisson-Voronoi tessellation of the plane, *J. Statist. Comput. Simul.*, **67**, 351–358.
- HINDE, A. L. and MILES, R. E. (1980) Monte Carlo estimates of the distributions of the random polygons of the Voronoi tessellation with respect to a Poisson process, *J. Statist. Comput. Simul.*, **10**, 205–223.
- KIANG, T. (1966) Random fragmentation in two and three dimensions, *Z. Astrophys.*, **64**, 433–439.
- KUMAR, S., KURTZ, S. K., BANAVAR, J. R. and SHARMA, M. G. (1992) Properties of a three-dimensional Poisson-Voronoi tessellation: a Monte Carlo study, *J. Statist. Phys.*, **67**, 523–551.
- MEIJERING, J. L. (1953) Interface area, edge length, and number of vertices in crystal aggregates with random nucleation, *Philips Research Rep.*, **8**, 270–290.
- MILES, R. E. (1970) On the homogeneous planar Poisson point process, *Mathematical Biosciences*, **6**, 85–127.
- MØLLER, J. (1994) *Lectures on Random Voronoi Tessellations*, Springer, New York.
- OKABE, A., BOOTS, B., SUGIHARA, K. and CHIU, S. N. (2000) *Spatial Tessellations: Concepts and Applications of Voronoi Diagrams*, 2nd Ed., John Wiley & Sons, Chichester.
- TANEMURA, M. (1988) Random packing and random tessellation in relation to the dimension of space, *J. Microscopy*, **151**, 247–255.
- TANEMURA, M., OGAWA, T. and OGITA, N. (1983) A new algorithm for three-dimensional Voronoi tessellation, *J. Computational Phys.*, **51**, 191–207.